Nano World Journal

https://doi.org/10.17756/nwj.2023-s5-076

Research Article

Open Access

Green Synthesis of Neem-based Zinc Oxide and Titanium Dioxide Nanoparticles for Enhanced Antimicrobial Functionalization of DBD Plasma Treated Silk and Corn Fabrics

Mumal Singh[1], Mona Vajpayee[2], Lalita Ledwani[1*] and Sudhir Kumar Nema[2]

[1]Department of Chemistry, School of Basic Sciences, Manipal University, Jaipur, Rajasthan, India

[2]HBNI, FCIPT, Institute for Plasma Research, Gandhinagar, Gujarat, India

[*]Correspondence to:
Lalita Ledwani
Department of Chemistry,
School of Basic Sciences,
Manipal University,
Jaipur, Gujarat, India.
E-mail: lalita.ledwani@jaipur.manipal.edu;
lalitaledwani@gmail.com

Received: October 20, 2023
Accepted: December 22, 2023
Published: December 28, 2023

Citation: Singh M, Vajpayee M, Ledwani L, Nema SK. 2023. Green Synthesis of Neem-based Zinc Oxide and Titanium Dioxide Nanoparticles for Enhanced Antimicrobial Functionalization of DBD Plasma Treated Silk and Corn Fabrics. *NanoWorld J* 9(S5): S461-S468.

Copyright: © 2023 Singh et al. This is an Open Access article distributed under the terms of the Creative Commons Attribution 4.0 International License (CCBY) (http://creativecommons.org/licenses/by/4.0/) which permits commercial use, including reproduction, adaptation, and distribution of the article provided the original author and source are credited.

Published by United Scientific Group

Abstract

Bacterial infectious diseases pose significant health and socio-economic challenges, necessitating the development of novel antimicrobial agents. Incorporating antimicrobial properties into textile materials is a promising approach, achieved through chemical or physical means. To enhance durability against washing treatments, environmentally friendly plasma surface modification has gained popularity as it selectively targets fabric surfaces without affecting their bulk properties. This research focuses on the green synthesis of zinc oxide (ZnO) and titanium dioxide (TiO_2) nanoparticles (NPs) using *Azadirachta indica* (Neem) leaves extract as a bio-reducing agent. The NPs are characterized using various techniques, including Fourier-transform infrared spectroscopy (FTIR), ultraviolet-visible (UV-Vis) spectroscopy, scanning electron microscopy coupled with energy dispersive X-ray spectroscopy (SEM-EDX), X-ray diffraction (XRD) analysis. The antibacterial efficacy of the synthesized NPs is evaluated against *Staphylococcus aureus* and *Escherichia coli*. Furthermore, the NPs are applied to silk and corn fabrics activated by dielectric barrier discharge (DBD) plasma. The antibacterial performance of these fabrics is assessed, highlighting their potential for applications in the fabric industry, particularly in the hygiene product sector.

Keywords

Dielectric barrier discharge plasma, Zinc oxide, Titanium oxide, Antibacterial, Neem leaves

Introduction

Metal nanomaterials have been the talk of the scientific world since they were discovered in 1959, and they have sustained their popularity until now. A nanoparticle can be defined as any particle with a dimension of 1-100 nm. These tiny particles have a range of applications in fields like engineering, medicine, optical, food, and recently in textiles [1]. Although many inorganic metals have semiconducting properties, ZnO and TiO_2 NPs are particularly interesting because they are non-toxic, cheap, and possess antimicrobial activity, antifungal activity, wound healing properties, UV blocking properties, high photocatalytic activity [1, 2]. The traditional methods used to synthesize these NPs often involve chemicals and consume energy which may prove to be environmentally polluting and may be harmful to our health. In the last decade, intensive study has been carried out on synthesizing metal NPs by green methods, be it from plants, bacteria, algae, or enzymes, to curb the chemical load on the environment and make them cheaper and eco-friendly [1, 3, 4].

Plant extracts derived from leaves, stems, roots, bark, or any other plant part have become a sustainable source of bioactive compounds that could facilitate

the synthesis of metal NPs. The chemicals in these extracts act as significant reducing, capping, or hydrolytic agents, making them capable of converting metal precursors into NPs under mild reaction conditions. ZnO and TiO_2 NPs are particularly valuable due to their chemical properties and ability to combat various microorganisms. As a result, they have found applications as antimicrobial agents in textile materials [3, 5]. These inherent qualities can significantly improve the functionality of textiles. *A. indica*, commonly known as 'neem' in India, belongs to the Meliaceae family. It is a native tree of the Indian subcontinent and has been used in Ayurvedic medicines for a long time due to its antimicrobial properties. *A. indica* contains various phytochemicals like flavonoids, terpenoids, phenols, saponins, alkaloids, and vitamins, out of which terpenoid azadirachtin, discovered first in 1960, is a known insecticide. The leaves of *A. indica* are known to possess antibacterial, antifungal, anti-inflammatory, antioxidant, anti-diarrheal, and anti-ulcer properties [1, 5, 6].

The textile material used in this study is ahimsa silk and corn fabrics, made of protein and cellulosic components, respectively. The ahimsa silk fiber is prepared from the mulberry silk moth cocoon without killing them, and the corn fiber is produced from the waste of corn crops, i.e., corn husk. Thus, both these fabrics are environmentally friendly. However, the main challenge faced while using natural fibers for any application is their hydrophobic nature, affecting the uniform attachment of any bioactive compound on their surface. To address this issue, researchers have recognized DBD plasma treatment as a technique for modifying textile surfaces. This allows the surface functionalization of fibers without affecting their bulk properties. The activated plasma species generated, whether in the air or any other noble gas like neon, helium, and argon, enable a variety of surface processes like surface etching or removal of surface contaminants, surface activation by breaking of bonds to generate active sites, and grafting of molecules or functional groups with the aid of monomer gases. This, in turn, enhances the surface roughness, wetting, and adhesion properties of the fabric and facilitates the penetration of nanoparticles into the structure of the fabric. Consequently, it enhances the durability and effectiveness of coatings [7, 8].

This research investigated the biological synthesis of ZnO and TiO_2 NPs using *A. indica* leaf extracts as reducing and stabilizing agents. The morphology, crystalline structure, phase, and size of NPs were characterized by XRD, UV-Vis spectroscopy, and SEM-EDX analysis. The synthesized NPs were then coated on silk and corn fabrics treated with 4 min of DBD plasma. The antimicrobial activity of the coated fabrics was studied by Agar diffusion test against test organism *S. aureus* and *E. coli*. The combination of these NPs with modified fabric surfaces has the potential to provide outstanding antimicrobial activity to textiles. To the best of our knowledge, no study has been conducted to investigate the antimicrobial potential of these modified nanoparticles on DBD plasma-treated silk and corn fabrics. This research aims to develop an environmentally friendly process to activate textile surface using plasma and nano-metal oxides modified with *A. indica* leaf extract that enhances the functionality and value of textiles. It also addresses concerns related to contamination and environmental sustainability.

Materials and Methods

Materials

A. indica (neem) leaves were collected from the campus of Manipal University Jaipur (Rajasthan, India). The leaves were washed with double-distilled water, dried in the shade, ground in fine powder, and stored for further use. Zinc nitrate hexahydrate and citric acid were purchased from Himedia, Titanium(IV) isopropoxide and ethanol absolute were purchased from Merck, India Pvt. Ltd. Degummed ahimsa silk fabric with 0.26 mm thickness was purchased from Herbal Fab, Gujarat, India. Corn fabric with 0.13 mm thickness was purchased from Aerations Company, Jaipur, Rajasthan. Fresh cultures of *S. aureus* (MTCC9542) and *E. coli* (MTCC10536) were used as the test microorganisms. The antibiotic used was levofloxacin.

Synthesis of ZnO NPs

10 g of dried neem leaves were boiled in 100 ml of autoclaved double distilled water at 60 °C for one hour. A yellow-colored *A. indica* leaf extract was filtered with Whatman filter paper no. 1 and kept at 4 °C for future use. ZnO NPs were synthesized by the previously reported method with some modifications [5]. 2 g zinc nitrate hexahydrate was added to 20 ml of this leaf extract while constantly stirring on a magnetic stirrer. The solution was then heated to 80 °C until it formed a deep yellow-greenish paste. The paste was then transferred to a silica crucible and calcined in a muffle furnace at 400 °C for two hours. The off-white powder obtained was used for further analysis.

Synthesis of TiO_2 NPs

15 g of dried *A. indica* leaf powder was boiled in 50 ml of sterilized double distilled water at 60 °C for one hour. The resulting extract was then filtered and stored for further experiments [9]. To create a TiO_2 precursor solution, 3 ml of titanium isopropoxide was added drop by drop to 20 ml of ethanol while stirred magnetically. One ml of *A. indica* plant extract was added to the precursor solution, which was continuously stirred and heated for three hours, resulting in a light-yellow colored paste. The paste was then dried in an oven at 100 °C until completely dry and cooled to room temperature. The dried powder was calcined in a muffle furnace at 600 °C for two hours to ensure complete oxidation. The resulting white TiO_2 NPs was ground into a fine powder with a mortar and pestle and stored in an airtight container.

Characterization techniques

Various characterization techniques assessed the ZnO NPs, and TiO_2 NPs synthesized through plant mediation. The NPs synthesis was preliminarily confirmed using a UV-Vis spectrophotometer (Shimadzu UV-2600, Japan). The functional groups involved in the bio-reduction and capping of ZnO NPs and TiO_2 NPs were identified using FTIR (Alpha FTIR spectrometer, Bruker, Germany) in the range of 4000 - 600cm^{-1}. The SEM (JEOL make JSM-7610FPlus, Japan) technique was used to assess the surface morphology of the synthesized NPs. The EDX spectroscopy was used to analyze the elemental content in the NPs. XRD analysis was performed on an X-ray diffractometer (SmartLab, Rigaku) operated at 40 kV and 50 mA. The pattern, which was recorded

by Cu-Kβ radiation, was employed with a scanning rate of 10°/min and step width of 0.02° from 2θ range of 20° to 80° to determine the crystallinity, purity, and size of the NP.

Plasma treatment of silk and corn fabric

The experiment used a rectangular Atmospheric Pressure Dielectric Barrier Discharge plasma system procured from Arshad Electronic Pvt. Ltd, Mumbai, India. The plasma chamber has dimensions 400mm×400mm×300mm and is surrounded by acrylic sheets. The fabrics were placed on a lower acrylic sheet covered with wire mesh and dielectric polyester (PET) film. Atmospheric air was used to treat the fabrics, with a DC voltage of 3kV and a current of 200mA. The fabric samples were cut to 1 x 1 cm^2 and treated for 4 min. The samples were tested right after plasma treatment. Details about the DBD plasma setup have been mentioned in the paper [10].

Coating of ZnO NPs and TiO_2 NPs on fabrics

The silk and corn fabrics were cut into small pieces measuring 1 x 1 cm^2. They were then treated with DBD plasma for four minutes. The duration of the treatment and other parameters for silk and cellulosic fabrics were optimized in previous studies [10, 11]. Next, the fabric samples were dipped into 1% NPs solutions with 5% citric acid as a binding agent. The mixture was sonicated for one hour at room temperature. Afterward, the fabrics were left to dry at room temperature and then cured at 80 °C for five minutes [1]. The same procedure was followed for coating fabrics with 5% plant extract.

Antibacterial assessment of NPs-coated fabrics

The Agar diffusion method determined the antibacterial activity of NPs and fabric coated with ZnO NPs and TiO_2 NPs. This quick and semi-quantitative test is effective in determining antibacterial activity. Samples were tested against *E. coli* (Gram-negative) and *S. aureus* (Gram-positive) strains. For the disc, the antibacterial activity of ZnO NPs (1 mg/ml) and TiO_2 NPs (1 mg/ml) were evaluated against levofloxacin as the positive control and sterile disc as the negative control and compared with 5% neem leaf extract. In the case of fabrics, the inhibition zone was compared between untreated and plasma-treated samples coated with plant extract and nanoparticles. A control plate was evaluated separately with untreated fabric and antibiotic-coated fabric.

Bacteria were grown in nutrient broth and spread on agar plates. Fabrics and sterile discs (6 mm) impregnated with NPs solution were placed on the streaked plates. These plates were then incubated at 37 °C overnight to observe the antibacterial activity of ZnO NPs and TiO_2 NPs and NPs-coated silk and corn fabric. The extent of the zone of inhibition (ZOI) produced around the sample served as an indication of the inhibitory effect of the compound on a particular microorganism. The ZOI is where bacterial growth is inhibited or prevented due to the compound's bacteriostatic effect [1, 7].

Results and Discussion

Qualitative and quantitative phytochemical analysis of neem leaf extract

The phytochemical screening of *A. indica* leaf extract was carried out to confirm the presence of primary classes of plant compounds like alkaloids, terpenoids, flavonoids, tannins, saponins, phenols, and reducing sugars, present in the aqueous, methanolic and water-methanol (1:1) solution. The results demonstrated that phyto-actives were present in all polarities of crude *A. indica* leaf extract but in varying strengths [12]. Antimicrobial and medicinal properties of plant extracts are associated with these secondary metabolites in many studies [13, 14]. These studies regarded the flavonoid-quercetin [15, 16] and terpenoid-azadirachtin [17, 18] to be mainly responsible for the antimicrobial activity of *A. indica* leaf extract. The presence of these compounds in the aqua methanolic extract was confirmed by high performance liquid chromatography (HPLC) analysis (Table 1) (Supplementary Data).

Table 1: Biochemical screening of phytoconstituents present in *A. indica* leaf extract [12].

S. No.	Biochemical test	Methanolic extract	Water:Methanol (1:1) extract	Aqueous extract
1	Test for alkaloids	++	+++	+
2	Test for flavonoids	++	+++	+
3	Test for terpenoids	++	+++	+
4	Test for tannins	++	++	++
5	Test for polyphenols	++	++	++
6	Test for reducing sugar	++	+++	+
7	Test for saponins	+	++	+++

Note: + : Low concentration, ++ : Moderate concentration, +++ : High concentration.

UV-Vis analysis of NPs

UV-Vis absorption spectroscopy technique is widely used to examine the optical properties of NPs at wavelengths ranging from 200 - 800 nm [1, 3]. The UV-Vis absorption spectra of ZnO and TiO_2 NPs were recorded at room temperature and shown in figure 1. Both ZnO and TiO_2 NPs were dispersed in water at 0.1% concentration. The UV-Vis absorption spectra show a characteristic peak at 370 nm for ZnO NPs and 360 nm for TiO_2 NPs, which matches the absorption spectrum of NPs synthesized by chemical methods and other plant extracts [2, 3, 4, 5, 19]. This absorption occurs due to the transition of electrons from the valence band to the conduction band [20].

The optical band gap of both the bio-synthesized NPs was calculated using the Tauc's plot, which goes by equation 1.

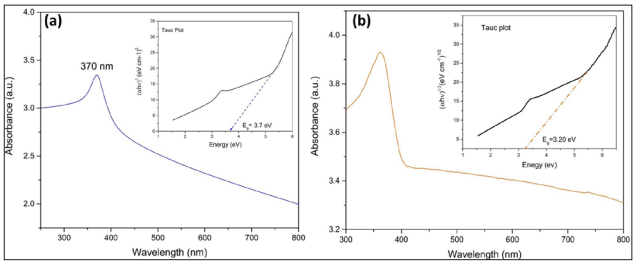


Figure 1: UV-Vis absorption spectra of **(a)** ZnO and **(b)** TiO_2 NPs.

$$(\alpha h\nu)^{\frac{1}{n}} = k(h\nu - E_g) \quad (1)$$

Where α = Extinction coefficient, $h\nu$ is the photon energy, K = constant, E_g = band gap energy, and n is an exponent which depends on the type of transition, n = 1/2 for indirect allowed transition and n = 2 for direct allowed transition.

The anatase TiO_2 NPs is an indirect band gap n-type semiconductor, whereas the hexagonal wurtzite ZnO NPs is a direct band gap semiconductor [2, 21, 22]. The band gap energy of ZnO NPs was found to be 3.7 eV, and that of TiO_2 NPs was 3.2 eV. The band gap energy of TiO_2 NPs matches that of bulk TiO_2 (3.22 eV) reported in many literatures [3, 19]. The band gap energy of ZnO NPs was higher than that of bulk ZnO (3.37 eV). This increase in energy could be explained based on the quantum confinement effect, where the band gap energy increases on the decrease of particle size [2, 23]. This effect arises when the NPs size is very small (less than 10 nm) and has a high surface-to-volume ratio, enhancing the quantum confinement effect and thus widening the band gap [20].

FTIR analysis

Figure 2a shows the FTIR spectra of *A. indica* leaf extract. The broad peak at 3318 cm^{-1} corresponds to the O-H stretching of polyols, peak at 2984 and 2832 cm^{-1} corresponds to C-H stretching of the carbon chain, peak at 1644 cm^{-1} depicts the C=C stretching vibrations of the aromatic ring, two small absorption bands at 1451 and 1408 cm^{-1} represents the bending vibrations of CH_2 and O-H of alcohols and carbonyl functional group, a sharp peak at 1015 cm^{-1} correspond to C-O stretching vibration of aromatic alcohols with a small peak at 1112 cm^{-1} of C-N stretching of amine. The peak at 562 cm^{-1} corresponds to the C-C stretching. These FTIR peaks show the presence of terpenoids, alkaloids, flavonoids, and phenolic compounds in the plant extract [2, 4, 5].

Figure 2b shows the FTIR spectrum of synthesized ZnO and TiO_2 NPs. A reduction in the intensity of the spectrum compared to plant extract indicates the active participation of plant metabolites in NPs synthesis. There is a slight shifting of peaks in the ZnO NPs spectra, with absorption at 3421 cm^{-1}, 1637 cm^{-1}, 1406 cm^{-1}, and 518 cm^{-1}. The peak at 518 cm^{-1} is the characteristic peak of Zn-O stretching vibrations [1, 2, 4, 5]. Similarly in figure 2c we can see peaks at 3225 cm^{-1}, 1624 cm^{-1}, 1437 cm^{-1}, 1000 cm^{-1}, 725 cm^{-1} and 524 cm^{-1} for TiO_2 NPs. The 3225 and 1624 cm^{-1} peaks indicate possible O-H stretching and -OH bending vibrations of adsorbed water molecules on the surface. The absorption bands at 725 and 524 cm^{-1} are the characteristic peaks of Ti-O-Ti stretching and Ti-O-O bonds [3, 20, 24]. From these spectra, it can be predicted that secondary metabolites present in leaf extract help in the bio-reduction of zinc and titanium precursors to ZnO and TiO_2 NPs where phenols, terpenoids and flavonoids play major roles. Also, the presence of C-N bonds in the spectra of synthesized NPs indicates the involvement of the amino group in forming a capping layer over the NPs surface. The free amino and carboxylic groups prevent agglomeration, and help stabilize the particles [4, 5, 25].

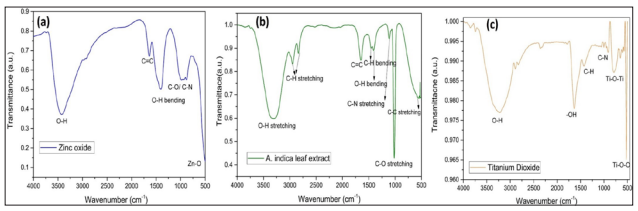


Figure 2: FTIR spectra of **(a)** ZnO NPs, **(b)** Leaf extract, and **(c)** TiO_2 NPs.

XRD analysis

Powder XRD is a quick and reliable technique for determining structural analysis like crystallite size, material phase, and unit cell dimension. The XRD diffraction pattern of ZnO NPs and TiO_2 NPs is shown in figure 3. The detected XRD pattern corresponds to the hexagonal phase (wurtzite structure) of ZnO NPs with lattice planes at (100), (002), (101), (102), (110), (103), (200), (112) and (201) values and anatase phase for TiO_2 at h, k, l lattice planes of (101), (004), (200), (105), (204), (220) and (301). The diffraction peaks were confirmed with the JCPDS file no-70-8072 and 64-0863, respectively [1, 3, 4, 5].

The XRD patterns of ZnO show intense and narrow peaks indicating that the synthesized NPs is crystalline. In contrast, in TiO_2, we observed broad peaks suggesting semicrystalline nature but with a smaller particle size [25].

The average crystalline size of biosynthesized NPs was determined using the Debye-Scherrer equation, which is given in equation 2.

$$D = K\lambda(\beta\cos\theta) \quad (2)$$

Where, D is the crystallite size, K is a constant with a value of 0.9, λ is X-ray wavelength, β is full width at half maxima, θ is the diffraction angle [2, 3, 4]. The calculated average crystallite size of the ZnO NPs was 20.42 nm, and for TiO_2 NPs, it was 5.03 nm.

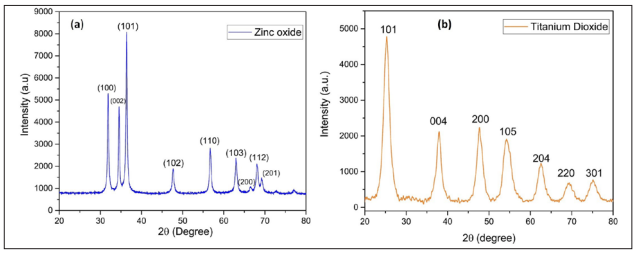


Figure 3: XRD diffraction spectra of **(a)** ZnO and **(b)** TiO_2 NPs.

SEM and EDX analysis

The surface morphology of ZnO and TiO_2 NPs was examined under SEM. The SEM images of the nanopowder are given in figure 4. The images depict the spherical shape of both biosynthesized NPs with less variation among particle sizes. The size of ZnO NPs varies from 19 - 28 nm correlating the size prediction by XRD analysis. In the case of TiO_2 NPs,

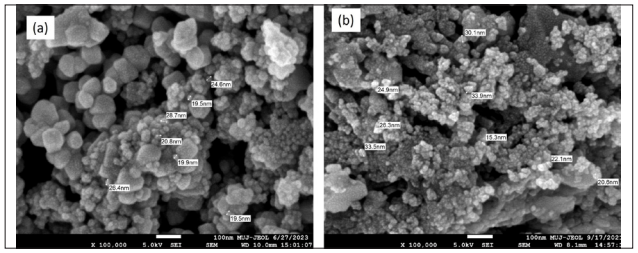


Figure 4: SEM micrograph of bio-synthesized **(a)** ZnO and **(b)** TiO_2 NPs.

the size variation is from 15 - 30 nm. The difference in the average size of TiO_2 NPs could be due to the agglomeration of nano-size particles. When the synthesis of metal NPs is carried out in aqueous media, cluster formation may also occur due to the high surface energy of metal oxide NPs [5]. Various literature studies have reported a similar size range for ZnO and TiO_2 NPs synthesized by the green route [1, 5, 6, 24]. According to reports, agglomerated particles are primarily utilized in electrochemical and biological applications [3, 26].

The elemental composition of synthesized nanopowder of ZnO and TiO_2 was studied by EDX analysis. Figure 5 depicts the EDX spectra of both nanostructures synthesized from *A. indica* leaf extract. We can confirm the formation of pure nanostructures from figure 5 as only the peaks of zinc, titanium, and oxygen elements are seen. The spectra eliminate the possibility of impurities as no other peak is observed except for gold used for coating.

Antibacterial study of biosynthesized ZnO and TiO_2 NPs on silk and corn fabric

The antibacterial activity of biosynthesized ZnO and TiO_2 NPs was studied against *E. coli* (Gram-negative) and *S. aureus* (Gram-positive) microbes using disc diffusion and well diffusion method. The experiment was repeated three times, and the mean value of the ZOI was reported. The ZOI is studied by measuring the area around a sterile disc or a well where there is absolutely no growth of bacteria, and the values were reported in cm. The antibacterial activity of biosynthesized NPs was compared with that of *A. indica* crude leaf extract, a positive control (levofloxacin) and a negative control (disc/sterile water). The results are shown in figure 6 for ZnO and figure 7 for TiO_2 NPs.

It can be observed from the agar plate and ZOI bar chart that the positive control gave the maximum ZOI and no zone in the negative control, as expected. The mean ZOI values of ZnO and TiO_2 NPs were noticeably more significant than that of crude leaf extract against both the microbes, with a difference of about 25% for ZnO and 40% for TiO_2 NPs.

The toxic effects of metal NPs on various microbes depend on their small size, resulting in close contact with the bacterial cell membrane. Extensive research has been carried out to decipher the mode of action of bacterial killing by metal nanostructures [2, 27, 28]. All the reported mechanisms point towards a single point, i.e., a change in the electrostatic potential of bacterial cell walls [29]. Most bacteria carry negative surface charge, and metal NPs function in two ways: by releasing positively charged metal ions line Zn^{+2} or Ti^{+2}

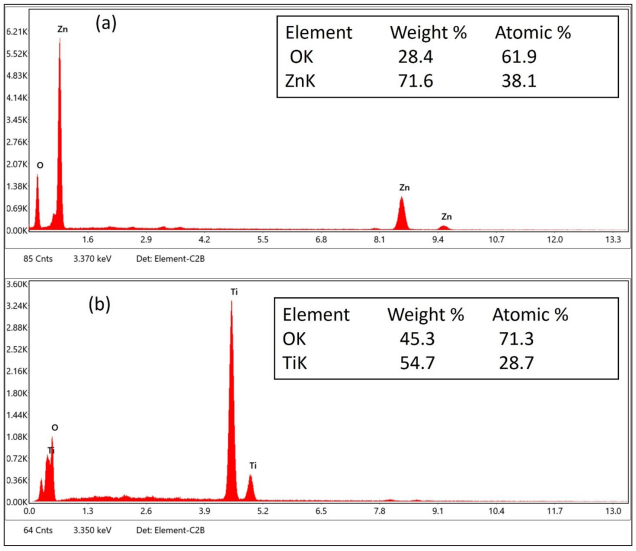


Figure 5: EDX spectra of **(a)** ZnO and **(b)** TiO_2 NPs.

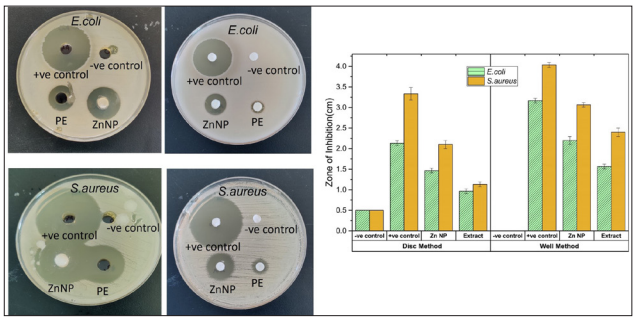


Figure 6: Antimicrobial activity of ZnO NPs against *E. coli* and *S. aureus* with the ZOI values.

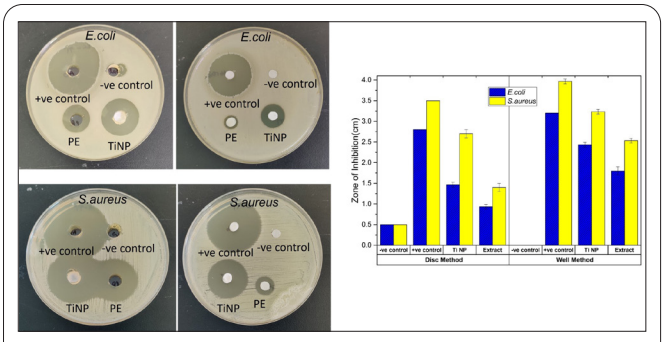


Figure 7: Antimicrobial activity of TiO_2 NPs against *E. coli* and *S. aureus* with the ZOI values.

or by generating reactive oxygen species (ROS) like H_2O_2, O_2^- on the NPs surface. The ROS/metal ions affect the zeta potential, disrupting the bacterial cell membrane permeability and leading to easy penetration of H_2O_2/metal ions inside. The ROS disrupts the electron transport chain or damages the DNA and membrane protein leading to cell death [1, 2, 3, 5].

In addition, we observed that *S. aureus* is more sensitive towards the nanostructure than *E. coli*. The *S. aureus* microbe is spherical with a single membrane, whereas *E. coli* is rod-shaped and double-membraned [10]. Thus, the ROS can penetrate faster and better in the single membraned microbe

leading to their death. The efficacy of nanostructures is more in comparison to crude plant extract. A possible reason for this is the size factor, where NPs being smaller in size, have a larger surface-to-volume ratio, thus able to attach to the bacterial cell membrane. In contrast, large-sized secondary plant metabolites of *A. indica* leaf extract cannot enter the cell membrane [5].

To utilize this antimicrobial potential of ZnO and TiO_2 NPs, we coated the silk and corn fabric with a 5 mg/ml NPs solution. The NPs-coated sample was tested against *E. coli* and *S. aureus* to check their efficacy using the agar plate method. The ZOI values for untreated (UT) and 4 min DBD plasma treated (PT) silk and corn samples coated with ZnO and TiO_2 NPs and plant extract (5%) are shown in figure 8 and figure 9, respectively.

In confirmation with the antimicrobial results obtained in the disc and well diffusion method, the inhibition zone values are higher for NPs than Plant extract coated fabrics with a difference of about 30% with ZnO and 40% with TiO_2 in bacterial reduction. On comparing the activity of UT with PT fabric, we can see that PT fabric shows better antibacterial activity when coated with plant extract and NPs.

The effect of DBD plasma treatment is more pronounced as the plasma activation of material leads to the attachment of free radicals and oxygen species on the fabric surface, rendering it more hydrophilic. A detailed study of the effect of DBD plasma treatment on silk and cellulose fabric has been previously carried out and reported [10, 11]. An increase in the wettability of the textile causes nanostructures to quickly penetrate the substrate medium, thus leading to enhanced attachment with microbial surface and, hence cell killing. Therefore, metal NPs synthesized by the green route can be used as an effective antimicrobial agent on natural fibers in medicinal applications and textile industry.

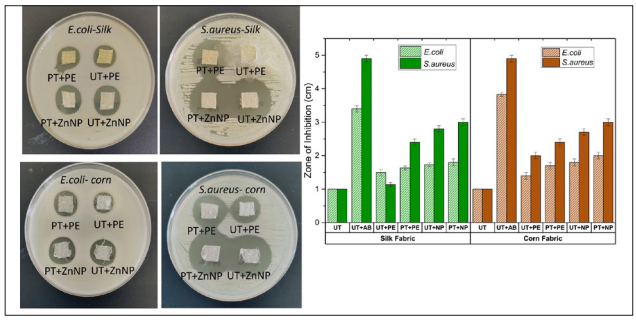


Figure 8: Antimicrobial activity of ZnO NPs coated silk and corn fabric against *E. coli* and *S. aureus* with the ZOI values.

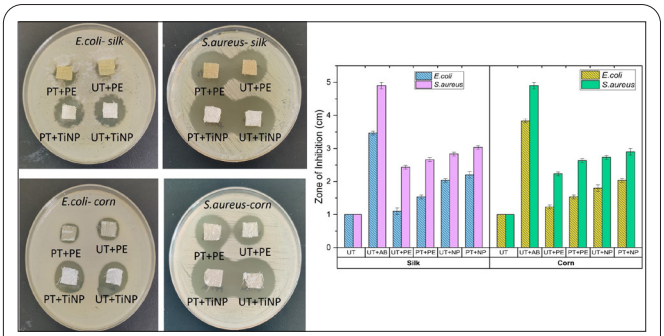


Figure 9: Antimicrobial activity of TiO_2 NPs coated silk and corn fabric against *E. coli* and *S. aureus* with the ZOI values.

Conclusion

In the present study, a simple, economical, and eco-friendly approach has been adopted for the biological synthesis of ZnO and TiO_2 NPs from the crude *A. indica* leaf extract. FTIR analysis confirmed that the water-soluble flavonoids, phenols, and amino groups acted as effective reducing and stabilizing agents. The synthesized ZnO and TiO_2 NPs were crystalline and were of hexagonal and anatase structure confirmed by XRD analysis. The band gap energy of 3.7 eV and 3.22 eV were obtained from Tauc's plot calculations. The SEM-EDX analysis confirmed the purity of the prepared NPs along with depicting the spherical shape, slight aggregation, and size, which varied from 19 - 28 nm for ZnO and 15 - 30 nm for TiO_2 NPs. The ZnO and TiO_2 NPs showed excellent antimicrobial activity against *E. coli* and *S. aureus* microbes on discs and PT silk and corn fabric. DBD plasma treatment enhanced the activity of green NPs by 20 - 30%. Thus, it can be concluded from the above details that using environmentally friendly green technologies like DBD plasma treatment and biosynthesized NPs can synergistically minimize the risk of infections against common pathogenic bacteria. These methods can be incorporated into the medical and textile industries to produce antimicrobial products.

Supplementary Data

Phytochemical tests

Qualitative phytochemical analysis was conducted for the detection of important secondary metabolites in the aqueous, and alcoholic extract of Tulsi (*O. sanctum*) and Green Tea (*C. sinensis*) leaves. The following test procedures were followed as reported in various reputed journals [30-32].

Test for alkaloids - Mayer's reagent test

3 ml of plant extract was treated with a few drops of dil. HCl and filtered. A few drops of Mayer's reagent were added to the filtrate to observe a creamy yellow precipitate of alkaloids.

Test for tannins and phenolic compound - Ferric chloride test

To 2 ml of plant extract solution, four drops of 5% ferric chloride solution were added. The solution turned bluish green, confirming the presence of tannins and phenolic compounds.

Test for terpenoids - Salkowski's test

5 ml of plant extract was mixed with 2 ml of chloroform. To this, 3 ml of conc. H_2SO_4 was added slowly from the side of the test tube. A reddish-brown layer was formed on the interface, confirming the presence of terpenoids.

Test for flavonoids - Alkaline reagent test

The extract was treated with a few drops of sodium

hydroxide solution separately in a test tube. The formation of intense yellow color, which becomes colorless with the addition of a few drops of dilute acid, indicated the presence of flavonoids.

HPLC analysis

HPLC Agilent 1260 infinite quaternary HPLC) equipped with DAD and RID detectors was used to identify the active ingredients in neem leaf extract. A reverse phase C-18 column was used for the chromatographic separation. To detect azadirachtin in *A. indica* extract, a chromatographic run was performed using a sample injection volume of 10 µl and a UV spectrophotometric detector set to 230 nm. The run lasted for 60 min. To achieve chromatographic separation, a stepwise gradient of two HPLC grade solvents, methanol and ultrapure milli Q water, was used. The solvents were passed through at a flow rate of 20 ml/min in the following sequence: methanol: water (70:30) for 40 min; methanol: water (80:20) for another 40 min; and methanol: water (90:10) for a final 20 min, with a 5-min delay between injections [33].

The HPLC analysis of *A. indica* leaves extracts revealed the presence of different phytoconstituents at different retention times. Standard identification was done under similar chromatogram conditions. For the HPLC analysis, methanol was used as one of the solvents along with milli Q water due to the natural constituents' extreme solubility in *A. indica* extracts and the ease of RP-C18 column. Figure 10 depicts the HPLC chromatogram of quercetin and azadirachtin standards along with *A. indica* leaves extracts. The HPLC analysis of quercetin and azadirachtin standards showed that quercetin separated at a retention time of 44.70 min, while azadirachtin separated at 5.39 min (Figures 10a and 10c). In the HPLC chromatogram of *A. indica* leave extract, peaks were obtained at the same retention time indicating the presence of quercetin and azadirachtin in the extract. The antibacterial properties of *A. indica* extract was attributed to the presence of flavonoid (Quercetin) and terpenoid (Azadirachtin) [33].

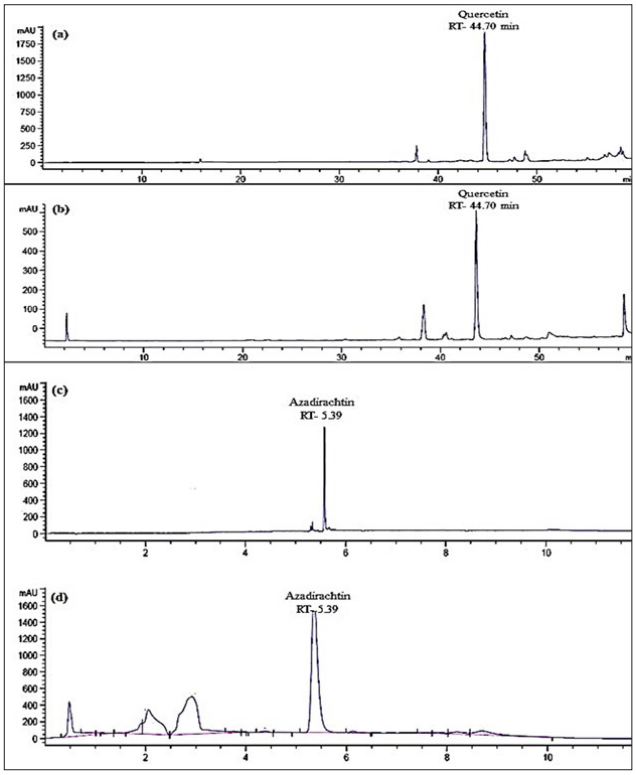


Figure 10: HPLC chromatogram of **(a)** standard - quercetin, **(b)** water-alcoholic extract of *A. indica* showing presence of quercetin, **(c)** standard - azadirachtin, and **(d)** water-alcohol extract of *A. indica* showing presence of azadirachtin.

Acknowledgements

The authors wish to thank Central Analytical Facility, Manipal University Jaipur for carrying out FTIR and U.V. analysis, Sophisticated Analytical Instrument Facility Manipal University Jaipur for carrying out SEM and XRD analysis.

Conflict of Interest

The authors declare that they have no known competing financial interests or personal relationships that could have appeared to influence the work reported in this paper.

Funding

None.

References

1. Sundrarajan M, Ambika S, Bharathi K. 2015. Plant-extract mediated synthesis of ZnO nanoparticles using *Pongamia pinnata* and their activity against pathogenic bacteria. *Adv Powder Technol* 26(5): 1294-1299. https://doi.org/10.1016/j.apt.2015.07.001
2. Bhuyan T, Mishra K, Khanuja M, Prasad R, Varma A. 2015. Biosynthesis of zinc oxide nanoparticles from *Azadirachta indica* for antibacterial and photocatalytic applications. *Mater Sci Semicond Process* 32: 55-61. https://doi.org/10.1016/j.mssp.2014.12.053
3. Ansari A, Siddiqui VU, Rehman WU, Akram MK, Siddiqi WA, et al. 2022. Green synthesis of TiO_2 nanoparticles using *Acorus calamus* leaf extract and evaluating its photocatalytic and *in vitro* antimicrobial activity. *Catalysts* 12(2): 181. https://doi.org/10.3390/catal12111451
4. Singh A, Kaushik M. 2019. Physicochemical investigations of zinc oxide nanoparticles synthesized from *Azadirachta Indica* (Neem) leaf extract and their interaction with Calf-Thymus DNA. *Results Phys* 13: 102168. https://doi.org/10.1016/j.rinp.2019.102168
5. Elumalai K, Velmurugan S. 2015. Green synthesis, characterization and antimicrobial activities of zinc oxide nanoparticles from the leaf extract of *Azadirachta indica* (L.). *Appl Surf Sci* 345: 329-336. https://doi.org/10.1016/j.apsusc.2015.03.176
6. Thakur BK, Kumar A, Kumar D. 2019. Green synthesis of titanium dioxide nanoparticles using *Azadirachta indica* leaf extract and evaluation of their antibacterial activity. *S Afr J Bot* 124: 223-227. https://doi.org/10.1016/j.sajb.2019.05.024
7. Irfan M, Hussain H, Saleem B, Saleem M, Shukrullah S, et al. 2022. Evaluation of ultrasonically ZnO loading effect on photocatalytic self-cleaning, UV protection and antibacterial activity of plasma/citric acid-activated cotton fabric. *Nanomaterials* 12(12): 2122. https://doi.org/10.3390/nano12122122
8. Shishoo R. 2007. Plasma Technologies for Textiles. Elsevier.
9. Venkatesh KS, Krishnamoorthi SR, Palani NS, Thirumal V, Jose SP, et al. 2015. Facile one step synthesis of novel TiO_2 nanocoral by sol-gel method using *Aloe vera* plant extract. *Indian J Phys* 89: 445-452. https://doi.org/10.1007/s12648-014-0601-8

10. Singh M, Vajpayee M, Ledwani L, Dave H, Nema SK. 2023. Study of physico-chemical and antibacterial properties of DBD plasma treated ahimsa silk coated with natural active agent. *Phys Scr* 98(6): 065001. https://doi.org/10.1088/1402-4896/accee2
11. Vajpayee M, Singh M, Ledwani L, Prakash R, Nema SK. 2020. Investigation of antimicrobial activity of DBD air plasma-treated banana fabric coated with natural leaf extracts. *ACS Omega* 5(30): 19034-19049. https://doi.org/10.1021/acsomega.0c02380
12. Vajpayee M, Dave H, Singh M, Ledwani L. 2022. Cellulase enzyme based wet-pretreatment of lotus fabric to improve antimicrobial finishing with *A. indica* extract and enhance natural dyeing: sustainable approach for textile finishing. *ChemistrySelect* 7(25): e202200382. https://doi.org/10.1002/slct.202200382
13. Wylie MR, Merrell DS. 2022. The antimicrobial potential of the neem tree *Azadirachta indica*. *Front Pharmacol* 13: 891535. https://doi.org/10.3389/fphar.2022.891535
14. Al-Hashemi ZS, Hossain MA. 2016. Biological activities of different neem leaf crude extracts used locally in Ayurvedic medicine. *Pac Sci Rev A Nat Sci Eng* 18(2): 128-131. https://doi.org/10.1016/j.psra.2016.09.013
15. Manikandan P, Letchoumy PV, Gopalakrishnan M, Nagini S. 2008. Evaluation of *Azadirachta indica* leaf fractions for *in vitro* antioxidant potential and *in vivo* modulation of biomarkers of chemoprevention in the hamster buccal pouch carcinogenesis model. *Food Chem Toxicol* 46(7): 2332-2343. https://doi.org/10.1016/j.fct.2008.03.013
16. Desai S, Tatke P, Gabhe S. 2017. Enhanced HPLC-DAD method for fast determination of quercetin-3-O-β-d-glucoside in extracts and polyherbal formulations containing *Azadirachta indica*—optimization and validation. *J Chromatogr Sci* 55(7): 706-711. https://doi.org/10.1093/chromsci/bmx024
17. Coventry E, Allan EJ. 2001. Microbiological and chemical analysis of neem (*Azadirachta indica*) extracts: new data on antimicrobial activity. *Phytoparasitica* 29: 441-450. https://doi.org/10.1007/BF02981863
18. Quelemes PV, Perfeito ML, Guimarães MA, dos Santos RC, Lima DF, et al. 2015. Effect of neem (*Azadirachta indica* A. Juss) leaf extract on resistant *Staphylococcus aureus* biofilm formation and *Schistosoma mansoni* worms. *J Ethnopharmacol* 175: 287-294. https://doi.org/10.1016/j.jep.2015.09.026
19. Saranya KS, Padil VVT, Senan C, Pilankatta R, Saranya K, et al. 2018. Green synthesis of high temperature stable anatase titanium dioxide nanoparticles using gum kondagogu: characterization and solar driven photocatalytic degradation of organic dye. *Nanomaterials* 8(12): 1002. https://doi.org/10.3390/nano8121002
20. Goutam SP, Saxena G, Singh V, Yadav AK, Bharagava RN, et al. 2018. Green synthesis of TiO_2 nanoparticles using leaf extract of *Jatropha curcas* L. for photocatalytic degradation of tannery wastewater. *J Chem Eng* 336: 386-396. https://doi.org/10.1016/j.cej.2017.12.029
21. Nagaraj G, Irudayaraj A, Josephine RL. 2019. Tuning the optical band gap of pure TiO_2 via photon induced method. *Optik* 179: 889-894. https://doi.org/10.1016/j.ijleo.2018.11.009
22. Luttrell T, Halpegamage S, Tao J, Kramer A, Sutter E, et al. 2014. Why is anatase a better photocatalyst than rutile? - Model studies on epitaxial TiO_2 films. *Sci Rep* 4(1): 4043. https://doi.org/10.1038/srep04043
23. Manzoor U, Islam M, Tabassam L, Rahman SU. 2009. Quantum confinement effect in ZnO nanoparticles synthesized by co-precipitate method. *Phys E Low Dimens Syst Nanostruct* 41(9): 1669-1672. https://doi.org/10.1016/j.physe.2009.05.016
24. Ahmad MZ, Alasiri AS, Ahmad J, Alqahtani AA, Abdullah MM, et al. 2022. Green synthesis of titanium dioxide nanoparticles using *Ocimum sanctum* leaf extract: *in vitro* characterization and its healing efficacy in diabetic wounds. *Molecules* 27(22): 7712. https://doi.org/10.3390/molecules27227712
25. Hudlikar M, Joglekar S, Dhaygude M, Kodam K. 2012. Green synthesis of TiO_2 nanoparticles by using aqueous extract of *Jatropha curcas* L latex. *Mater Lett* 75: 196-199. https://doi.org/10.1016/j.matlet.2012.02.018
26. Sankar R, Rizwana K, Shivashangari KS, Ravikumar V. 2015. Ultra-rapid photocatalytic activity of *Azadirachta indica* engineered colloidal titanium dioxide nanoparticles. *Appl Nanosci* 73173-73176. https://doi.org/10.1007/s13204-014-0369-3
27. Azizi-Lalabadi M, Ehsani A, Divband B, Alizadeh-Sani M. 2019. Antimicrobial activity of titanium dioxide and zinc oxide nanoparticles supported in 4A zeolite and evaluation the morphological characteristic. *Sci Rep* 9(1): 17439. https://doi.org/10.1038/s41598-019-54025-0
28. Jiang S, Lin K, Cai M. 2020. ZnO nanomaterials: current advancements in antibacterial mechanisms and applications. *Front Chem* 8: 580. https://doi.org/10.3389/fchem.2020.00580
29. Halder S, Yadav KK, Sarkar R, Mukherjee S, Saha P, et al. 2015. Alteration of zeta potential and membrane permeability in bacteria: a study with cationic agents. *SpringerPlus* 4: 672. https://doi.org/10.1186/s40064-015-1476-7
30. Mahendiran D, Subash G, Arumai Selvan D, Rehana D, Kumar RS, et al. 2017. Biosynthesis of zinc oxide nanoparticles using plant extracts of *Aloe vera* and *Hibiscus sabdariffa*: phytochemical, antibacterial, antioxidant and anti-proliferative studies. *BioNanoSci* 7(3): 530-545. https://doi.org/10.1007/s12668-017-0418-y
31. Mousavi L, Salleh RM, Murugaiyah V. 2018. Phytochemical and bioactive compounds identification of *Ocimum tenuiflorum* leaves of methanol extract and its fraction with an antidiabetic potential. *Int J Food Prop* 21(1): 2390-2399. https://doi.org/10.1080/10942912.2018.1508161
32. Tayade US, Borse AU, Meshram JS. 2018. First report on *Butea monosperma* flower extract based nickel nanoparticles green synthesis and characterization. *Int J Sci Res Sci Eng Technol* 4(3): 43-49.
33. Vajpayee M, Dave H, Singh M, Ledwani L. 2022. Cellulase enzyme based wet-pretreatment of lotus fabric to improve antimicrobial finishing with *A. indica* extract and enhance natural dyeing: sustainable approach for textile finishing. *ChemistrySelect* 7(25): 1-17. https://doi.org/10.1002/slct.202200382